 CMES, vol.66, no.2, pp.117-134, 2010

Geometric Formulation of Maxwell's Equations in the Frequency Domain for 3D Wave Propagation Problems in Unbounded Regions

P. Bettini[1], **M. Midrio**[2] **and R. Specogna**[2]

Abstract: In this paper we propose a geometric formulation to solve 3D electromagnetic wave problems in unbounded regions in the frequency domain. An absorbing boundary condition (ABC) is introduced to limit the size of the computational domain by means of anisotropic Perfectly Matched Layers (PML) absorbing media in the outer layers of an unstructured mesh. The numerical results of 3D benchmark problems are presented and the effect of the PML parameters and scaling functions on PML effectiveness are discussed.

Keywords: Electromagnetic wave propagation, Discrete Geometric Approach (DGA), Cell Method (CM), PML, ABC.

1 Introduction

In the last decades, several methods have been developed to numerically solve Maxwell's equations over a finite mesh: From the classical Finite Element Method (FEM) [Jin (1993)] and Finite-Difference Time-Domain (FDTD) [Yee (1966)], to Finite Integration Technique (FIT) [Weiland (1977, 1985)]. More recently, the so-called Discrete Geometric Approach (DGA)[3] gained popularity in Computational Electromagnetics [Tonti (1975, 1988, 2002); Bossavit (1998b); Bossavit and Kettunen (2000)]. According to this approach, the electromagnetic field is discretized over a pair of interlocked cell complexes. The unknowns of the problem are the circulations along edges and fluxes across faces, and they are arranged in degrees of freedom (DoF) arrays.

The DGA have been already applied as a numerical method to solve various classes of physical problems. In particular, a number of numerical routines have been

[1] Dipartimento di Ingegegneria Elettrica (DIE), Università degli Studi di Padova, Padova, Italy.
[2] Dipartimento di Ingegegneria Elettrica, Gestionale e Meccanica (DIEGM), Università degli Studi di Udine, Udine, Italy.
[3] Also referred to as Cell Method (CM).

developed to solve wave propagation problems on unstructured grids in the frequency domain, see for example [Weiland (1977); Teixeira and Chew (1999); Marrone (2001); Cinalli, Edelvik, Schuhmann, and Weiland (2004); Bettini, Boscolo, Specogna, and Trevisan (2006)]. Nevertheless, not so much has been done yet in the framework of the geometric formulations to tackle 3D wave propagation in unbounded regions (e.g. towards infinite free space around a scatterer/radiator or through waveguides with infinite length).

The aim of the present paper is that of extending the Discrete Geometric Approach of Maxwell's equations in the frequency domain to the case of unbounded regions, by introducing anisotropic Perfectly Matched Layers (PML) in the outer layers of an unstructured mesh [Taflove (1995)] to limit the size of the computational domain. Numerical results of 3D non trivial benchmark problems will be presented to validate the approach, and the effect of the PML parameters and scaling functions on the reflectionless absorption effectiveness will be discussed in details.

2 The Discrete Geometric Approach (DGA)

According to the DGA a pair of interlocked grids is introduced in the computational domain of interest D. We denote denote them as *primal* and *dual*, respectively. The primal mesh is tetrahedral, while the dual is obtained by the primal one by barycentric subdivision, see for example [Tonti (1998, 2002)]. The incidence matrices relative to the primal and dual interlocked grids form the cell complexes $\mathscr{K}$ and $\mathscr{B}$, respectively. The geometric elements of $\mathscr{K}$ are referred to n for nodes, e for edges, f for triangular faces and v for tetrahedra, whereas the geometric elements of the barycentric complex $\mathscr{B}$ are referred to $n_{\mathscr{B}}$, $e_{\mathscr{B}}$, $f_{\mathscr{B}}$ and $v_{\mathscr{B}}$, respectively. We denote the incidence matrices relative to $\mathscr{K}$ with $\mathbf{G}$ between edges e and nodes n, with $\mathbf{C}$ between faces f and edges e and with $\mathbf{D}$ between cells v and faces f. The matrices $\tilde{\mathbf{G}} = \mathbf{D}^T$, $\tilde{\mathbf{C}} = \mathbf{C}^T$ and $\tilde{\mathbf{D}} = -\mathbf{G}^T$ describe the incidences of the dual complex $\mathscr{B}$.

The integrals of the electromagnetic differential forms with respect to the oriented geometric elements of the pair of complexes $\mathscr{K}$ and $\mathscr{B}$ are referred to as Degrees of Freedom (DoFs) [Bossavit (1998a)]. Each DoF is stored in a DoFs array and indexed with the corresponding geometric element on which integration is performed. The DoFs arrays will be denoted in boldface type. According to the Tonti's classification of variables, there is a unique association between every physical variable and the corresponding oriented geometric element.

2.1 Geometric formulation in terms of U

For an electromagnetic wave propagation problem, the following arrays of DoFs are introduced:

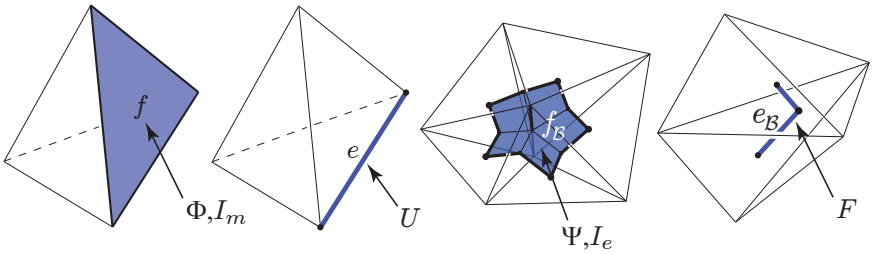

Figure 1: Association of the DoFs to the oriented geometrical elements.

- $\mathbf{\Phi}$ is the array of magnetic fluxes associated with faces $f \in \mathscr{K}$;
- $\mathbf{\Psi}$ is the array of electric fluxes associated with dual faces $f \in \mathscr{B}$;
- $\mathbf{F}$ is the array of magneto-motive forces (m.m.f.s) associated with dual edges $e_{\mathscr{B}} \in \mathscr{B}$;
- $\mathbf{I}_e$ is the array of source currents associated with dual faces $f_{\mathscr{B}} \in \mathscr{B}$;
- $\mathbf{U}$ is the array of electro-motive forces (e.m.f.s) on primal edges $e \in \mathscr{K}$.

We assume that no free charge is present in D and all the media are linear. The discrete Maxwell's equations [Tonti (1975); Weiland (1977)] are written as

$$\begin{aligned} &\mathbf{CU} = -\frac{d\mathbf{\Phi}}{dt} && (a)\\ &\mathbf{C}^T\mathbf{F} = \mathbf{I}_e + \frac{d\mathbf{\Psi}}{dt} && (b)\\ &\mathbf{D\Phi} = \mathbf{0} && (c)\\ &-\mathbf{G}^T\mathbf{\Psi} = \mathbf{0}, && (d) \end{aligned} \tag{1}$$

where (1a) is the Maxwell–Faraday's law, (1b) is the Ampère–Maxwell's law, (1c) is the magnetic Gauss's law and (1d) is the electric Gauss's law.

Continuity equation $-\mathbf{G}^T(\mathbf{I}_e + \frac{d\mathbf{\Psi}}{dt}) = \mathbf{0}$ is implied by (1b); from it and (1d) we have $\mathbf{G}^T\mathbf{I}_e = \mathbf{0}$.

The discrete counterparts of the constitutive laws, called constitutive matrices, are now considered. Constitutive matrices links the arrays of DoFs as

$$\begin{aligned} &\mathbf{F} = \boldsymbol{\nu}\mathbf{\Phi} && (a)\\ &\mathbf{\Psi} = \boldsymbol{\varepsilon}\mathbf{U}, && (b) \end{aligned} \tag{2}$$

where $\boldsymbol{\nu}$ and $\boldsymbol{\varepsilon}$ are square matrices depending upon the geometry of the problem and the parameters of the materials. The construction of the constitutive matrices is the topic of Section 2.2.

The discrete wave propagation problem in the frequency domain consists of determining the DoF arrays such that (1) and (2) are satisfied simultaneously [Tonti (1975); Weiland (1977)]. We may reformulate this problem in terms of DoF array $\mathbf{U}$ only. By assuming the magnetic currents null in D, by substituting in (1b), (2a) for $\mathbf{F}$, (2b) for $\mathbf{\Psi}$ and using (1a), we obtain a sparse linear system of equations

$$\mathbf{K}\mathbf{U} = -i\omega\mathbf{I}_e, \tag{3}$$

where

$$\mathbf{K} = \mathbf{C}^T\boldsymbol{\nu}\mathbf{C} - \omega^2\boldsymbol{\varepsilon}. \tag{4}$$

A synthetic tool that gives relevance to the geometrical aspects of the approach, and allows to derive the algebraic formulation of Maxwell's equations for wave propagation problems in the frequency domain, is the Tonti's diagram (for a comprehensive description, see [Tonti (1975)]), see Fig. 2.

2.2 Constitutive matrices and their construction

The square matrix $\boldsymbol{\nu}$ is the reluctance matrix[1] such that (2a) holds exactly at least for an element-wise *uniform* induction field B and magnetic field H in each cell and it is the approximate discrete counterpart of the constitutive relation $\mathrm{H} = \nu\,\mathrm{B}$ at continuous level, ν being the reluctivity assumed element-wise uniform.

The square matrix $\boldsymbol{\varepsilon}$ is the permittivity matrix[2] such that (2b) holds exactly at least for an element-wise *uniform* electric field E and electric flux density D in each cell and it is the approximate discrete counterpart of the constitutive relation $\mathrm{D} = \varepsilon\,\mathrm{E}$ at continuous level, ε being the permittivity assumed element-wise uniform.

A classical way to construct the constitutive matrices $\boldsymbol{\nu}$ and $\boldsymbol{\varepsilon}$ for a tetrahedral mesh is the technique based on Whitney maps described in [Tarhasaari, Kettunen, and Bossavit (1999)], where the resulting matrices are non-symmetric. The fact that matrices are non-symmetric is irrelevant for the reluctance matrix, while the permittivity matrix $\boldsymbol{\varepsilon}$ can be constructed in a symmetric way as described in [Specogna and Trevisan (2005)]. Alternatively, the Galerkin Hodge technique [Bossavit (2000)] produces the same stiffness and mass matrices as the Finite Elements with first order Whitney edge and face element basis functions. Another solution that guar-

[1] $\dim(\boldsymbol{\nu}) = N_f$, N_f being the number of faces in $\mathscr{K}$.
[2] $\dim(\boldsymbol{\varepsilon}) = N_e$, N_e being the number of edges in $\mathscr{K}$.

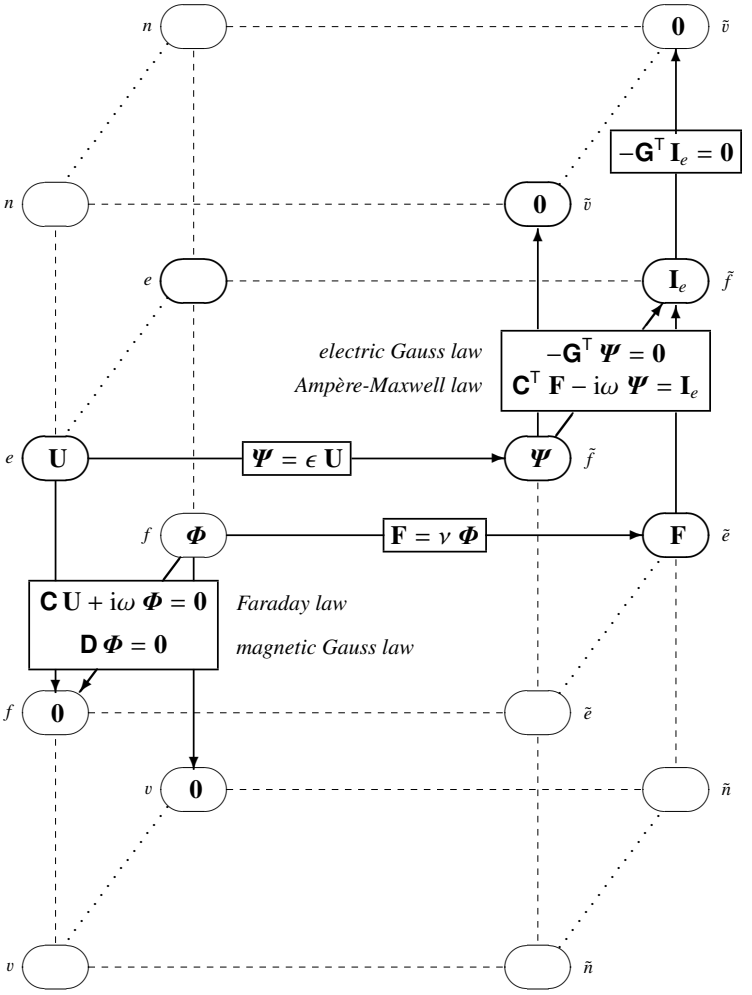

Figure 2: Tonti's diagram for wave propagation problems in the frequency domain. The pillars on the left refer to primal space and time complexes, the pillars on the right to their dual.

antees both stability and consistency[3] simultaneously exploits the original set of edge and face vector basis functions defined in [Codecasa, Specogna, and Trevisan (2007)] for tetrahedra and triangular prisms. In the case of hexahedral grids, the construction of the constitutive matrices can be addressed as in [Dular, Specogna,

[3] A precise definition of the notion of *consistency* for constitutive matrices is available in [Bossavit and Kettunen (2000)].

and Trevisan (2008)], where a consistent but non-symmetric matrix is obtained. To gain symmetry, at the price of consistency, the Galerkin Hodge technique can be used instead, by means of the mixed elements vector basis functions described in [Dular, Hody, Nicolet, Genon, and Legros (1994)]. In order to recover again stability and consistency simultaneously, the original geometric technique presented in [Codecasa, Specogna, and Trevisan (2008)] can be profitably used. Symmetric, positive-definite and consistent constitutive matrices suitable with a conformal mesh made by general polyhedra have been recently introduced in [Codecasa, Specogna, and Trevisan (2009a, 2010)]. The possibility of using general polyhedral elements, enables the rigorous use of *subgridding* [Codecasa, Specogna, and Trevisan (2009b)].

The keypoint of geometric-based construction of constitutive matrices is that no numerical evaluation of a volume integral is needed. In fact, the constitutive matrices can be constructed by using only the vectors associated with the geometric elements of the cell complexes $\mathscr{K}$ and $\mathscr{B}$, which yields to simple and computationally efficient solutions.

2.3 Boundary Conditions

When analysis of a propagating wave is considered, both in the time and frequency domain, Boundary Conditions (BCs) are needed to close the computation domain. However, so far DGA has been tested mostly by simulating the propagation of an electromagentic wave inside a hard-wall waveguide. To this end, simple Perfectly Electric Conductor (PEC) or Perfectly Magnetic Conductor (PMC) boundaries have been used. On the other hand, geometries of real interest are often defined in open regions, i.e in a domain (either 2D or 3D) which is unbounded with respect to at least one coordinate. In this case, suitable BCs must be introduced on the outer part of the computational domain to limit its size, while allowing outward propagating waves to exit without giving rise to unphysical reflections.

At this purpose, during the 1970s and 1980s a number of analytical techniques have been developed and implemented in FDTD computer softwares, from radiation operators [Bayliss and Turkel (1980); Bayliss, Gunzburger, and Turkel (1982); Higdon (1986, 1987)], one way wave equations [Engquist and Majda (1977)], extrapolation techniques [Liao, Wong, Yang, and Yuan (1984)], to Ramahi's complementary operator method (COM) [Ramahi (1997, 1998)].

In a different approach, the outer boundary of the computation domain may also be numerically coated with an artificial absorbing material. The main idea behind this approach is that of mimicking the superficial treatment of an anechoic chamber. This trick was first suggested by J.P. Berenger, who introduced a highly effective absorbing material, that he called *Perfectly Matched Layer* (PML), to truncate 2D

FDTD meshes [Berenger (1996)]. To this end, a novel split field formulation of Maxwell's equations was used by Berenger in his original paper. Later on, it was proved that an equivalent behavior could also be obtained by introducing a suitable complex stretched coordinate system into Maxwell's equations [Chew and Weedon (1994); Rappaport (1995)]. With both the approaches, a planar interface between the PML material and free space is reflectionless for plane waves of arbitrarily incidence, polarization and frequency.

In this paper we focus on yet a different approach, which is based on a physical model of the absorbing medium [Sacks, Kingsland, Lee, and Lee (1995)]. For a planar interface (between the anisotropic medium and free space) this medium has an uniaxial anisotropy and is described by means of electric permittivity and magnetic permeability tensors. Values in these tensors can be chosen such that the interface is perfectly reflectionless.

2.3.1 Uniaxial Perfectly Matched Layer (UPML)

The uniaxial medium (UPML) performs as well as Berenger's PML or its complex stretched coordinate counterpart, but it does not require a modification of Maxwell's equations. Therefore, its implementation into the DGA code is straightforward. in fact, DGA can easily handle anisotropies in the material's properties.

To illustrate the main idea behind the UPML approach, we begin with the simple 2D geometry of Fig.3. Later on, we will show the generalization to the full 3D case. An arbitrarily polarized time harmonic plane wave impinges on the planar interface between Region 1 (which is supposed to be a loss less, isotropic medium, half-space $x < 0$) and Region 2 (uniaxial PML medium, half-space $x > 0$).

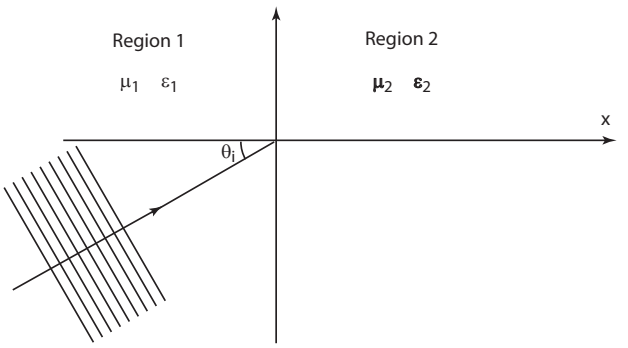

Figure 3: A plane wave incident upon a half-space of diagonal anisotropic medium.

By a proper decomposition of the plane wave into a linear combination of forward and backward TE_z (the electric field E has only a z-component) and TM_z (the magnetic field H has only a z-component) modes, it can be shown [Sacks, Kingsland, Lee, and Lee (1995)] that the planar interface is perfectly reflectionless for plane waves with arbitrary incidence, polarization and frequency, provided that the electric and magnetic tensors of the uniaxial PML read as follows

$$\boldsymbol{\varepsilon}_2 = \varepsilon_1 \boldsymbol{S_x}, \qquad \boldsymbol{\mu}_2 = \mu_1 \boldsymbol{S_x}, \qquad \boldsymbol{S_x} = \begin{bmatrix} s_x^{-1} & 0 & 0 \\ 0 & s_x & 0 \\ 0 & 0 & s_x \end{bmatrix}. \tag{5}$$

Notice that the reflectionless behavior at the interface is observed for any real or complex value of s_x. Indeed, this parameter does not affect the wave impedance of the field in the UPML medium, so that the reflectionless behavior is solely determined by the proper choice of the magnetic permittivity and electric permeability: $\sqrt{\mu_1 \varepsilon_1} = \sqrt{\mu_2 \varepsilon_2}$.

An interpretation on the material properties $(\mu, \varepsilon, \sigma_M, \sigma_E)$ required for a perfectly matched interface can be found in [Sacks, Kingsland, Lee, and Lee (1995)].

Usually, the following form is chosen for s_x: $s_x = 1 + \frac{\sigma_x}{i\omega\varepsilon_1}$. This way, the transmitted wave propagates in the UPML medium with the same phase velocity as the incident wave. Nevertheless, the imaginary part of the tensor gives rise to an attenuations which turns out to be independent of frequency, and dependent on the incidence angle θ_i and the magnitude of the conductivity σ_x.

Similar results can be obtained for planar interfaces in the other coordinate directions (y, z) too, so that a generalized 3D formulation of the UPML medium can be derived very simply [Taflove (1995)]. To this end, one defines 3D electric and magnetic tensors as follows:

$$\boldsymbol{\varepsilon}_2 = \varepsilon_1 \boldsymbol{S}, \qquad \boldsymbol{\mu}_2 = \mu_1 \boldsymbol{S}, \tag{6}$$

where $\boldsymbol{S}$ is the following diagonal matrix

$$\begin{aligned} \boldsymbol{S} = \boldsymbol{S_x}\,\boldsymbol{S_y}\,\boldsymbol{S_z} &= \begin{bmatrix} s_x^{-1} & 0 & 0 \\ 0 & s_x & 0 \\ 0 & 0 & s_x \end{bmatrix} \begin{bmatrix} s_y & 0 & 0 \\ 0 & s_y^{-1} & 0 \\ 0 & 0 & s_y \end{bmatrix} \begin{bmatrix} s_z & 0 & 0 \\ 0 & s_z & 0 \\ 0 & 0 & s_z^{-1} \end{bmatrix} = \\ &= \begin{bmatrix} \frac{s_y s_z}{s_x} & 0 & 0 \\ 0 & \frac{s_x s_z}{s_y} & 0 \\ 0 & 0 & \frac{s_x s_y}{s_z} \end{bmatrix}, \end{aligned} \tag{7}$$

and $s_\xi = k_\xi + \frac{\sigma_\xi}{i\omega\varepsilon_1}$, $\xi = \{x, y, z\}$[4].

[4] Values $k_\xi \neq 1$ still permit to achieve perfect impedance matching, while attenuating evanescent waves too.

As for the numerical implementation of UPMLs in the computational domain, one may proceed as follows. The domain is decomposed in an inner region, where the geometry of the real problem at hand are placed, along with the sources of the electromagnetic field, and an outer region, which is formed by 26 anisotropic subregions. 8 of those are trihedral corners, 12 are dihedral edges and 6 are boundary faces, as shown in Fig. 4.

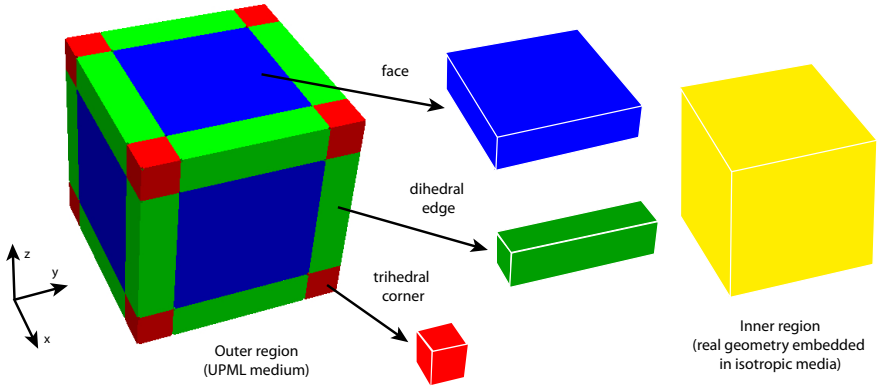

Figure 4: The computational domain is subdivided into an inner region (different sources are embedded in isotropic media) and an outer region which includes 26 anisotropic subregions (8 trihedral corners, 12 dihedral edges, 6 faces).

For the sake of simplicity, we assume that the inner region is homogeneous, so that its electric permittivity and magnetic permeability are constant and the generalized constitutive tensor $\boldsymbol{S}$ reduces to the identity matrix. Whereas, parameters of the electric and magnetic tensors in the 26 anisotropic boundary subregions are defined as follows:

- *Faces (6)*
  - UPML media at faces normal to $\hat{x}$: $\sigma_y = \sigma_z = 0$ and $k_y = k_z = 1$.
  - UPML media at faces normal to $\hat{y}$: $\sigma_x = \sigma_z = 0$ and $k_x = k_z = 1$.
  - UPML media at faces normal to $\hat{z}$: $\sigma_x = \sigma_y = 0$ and $k_x = k_y = 1$.
- *Dihedral edges (12)*
  - UPML media at dihedral edges normal to $\hat{x}$ and $\hat{y}$: $\sigma_z = 0$ and $k_z = 1$.
  - UPML media at dihedral edges normal to $\hat{x}$ and $\hat{z}$: $\sigma_y = 0$ and $k_y = 1$.

- UPML media at dihedral edges normal to $\hat{y}$ and $\hat{z}$: $\sigma_x = 0$ and $k_x = 1$.

- *Trihedral corners (8)*

  - UPML media at trihedral corners: the complete general tensor $\boldsymbol{S}$ is used.

2.3.2 Grading of the UPML loss parameters

In any practical implementation, the absorbing layer has a finite thickness L_{PML} and is terminated by the outer boundary of the mesh. Notice that since the task of UPMLs is exactly that of attenuating the outward-propagating waves, small fields components have to be expected in the outer boundary of the computational domain. This in turn means that no particular care has to be employed in their implementation, i.e. no radiation operators or extrapolation techniques need really to be used. Even a simple PEC wall can actually perform well enough. Indeed, the amplitude of a wave which travels through the UPML and is reflected by the hard wall and travels back again through the UPML into the computational domain is

$$R(\theta) = e^{-2\,\sigma_\xi\,\eta\,\cos\theta\,L_{PML}}, \tag{8}$$

where θ is the angle of incidence (with respect to the ξ-directed surface normal), and σ_ξ and η are, respectively, the PML's electric conductivity, referred to the propagation in the ξ-direction, and the characteristic wave impedance. We call $R(\theta)$ the theoretical *reflection error*. Poor performance, if any, may be expected for glancing incidence ($\theta \approx \pi/2$) only, while a rapid decay of the spurious reflected wave is usually obtained. Notice that, as it might actually be expected, the larger is the product $\sigma_\xi\,L_{PML}$, the smaller is the reflection error. From the viewpoint of the computational burden, this might induce to think that the use of a really thin UPML layer with a large conductivity value should be the right choice. Actually, the theoretically rigorous reflectionless behavior of UPMLs is affected by the mesh discretization error, and additional spurious reflections can arise if too abrupt discontinuities among domain parameters are present. Usually, therefore, a suitable grading of σ along ξ is required to balance the $R(\theta)$ and the mesh discretization error.

Several grading profiles have been suggested in the literature [Taflove (1995)]. In the present paper, the polynomial one ($2 \leq m \leq 4$) has been adopted

$$\sigma = \left(\frac{\xi}{d}\right)^m \sigma_{\xi,max}. \tag{9}$$

The following rule of thumb has proven to be effective to calculate the optimal value of $\sigma_{\xi,max}$

$$\sigma_{\xi,max} = q\,\frac{m+1}{\eta\,\Delta}, \tag{10}$$

where Δ is the average step size of the unstructured mesh in the ξ direction; typically $0.1 \leq q \leq 0.8$ has been found to be nearly optimum for most cases.

3 Numerical experiments

Correct implementation of UPMLs in the DGA has been checked through an extensive series of numerical experiments, that we performed on two benchmark problems: a rectangular waveguide and a $\lambda/2$ linear antenna. Observe that the choice for such simple problems was done on purpose: indeed, the focus of the present paper is the implementation of UPMLs in DGA in the presence of unstructured meshes and unlimited domain, not the characterization of the electromagnetic behavior of a given device. Simple benchmark problems gave us the possibility of checking the numerical results against analytical solutions. This way we could actually understand how the UPML parameters affect the accuracy of the solution. Observe also that the performance of UPML is almost independent on the complexity of the dielectrics and sources inside the computational domain (at least as long as the radiated field does not primarily impinges on the boundaries along very grazing rays). Therefore, our analysis may represent a useful guideline for the design of UPMLs in the DGA even in the presence of more complex electromagnetic problems.

3.1 Rectangular waveguide

We consider a rectangular waveguide with the width $a = 3\,cm$ and length $L = 5\,cm$ (see Fig. 5), at the operating frequency $f = 10\,\text{GHz}$. With these parameter, the wavelength of the guided wave turns out to be $\lambda_g = 3.46\,cm$. An electric source with the spatial profile of the TE_{10} mode is introduced at the input coordinate $z = 0$, while the anisotropic UPML is place at the opposite side (i.e. for $L \leq z < L + L_{PML}$). A PEC terminates the UPML at $z = L + L_{PML}$.

As a preliminary step, a 2D analysis has been performed in order to select the parameters of the anisotropic medium (UPML): thickness of the PML layer ($1\,cm \leq L_{PML} \leq 4\,cm$) and order of the polynomial profile of the electric conductivity ($2 \leq m \leq 4$) with its maximum value ($\sigma_{z,max}$), as optimized according to (10).

Later on, for any dyad (L_{PML}, m) the effect of the step size (Δh_z) within the UMPL

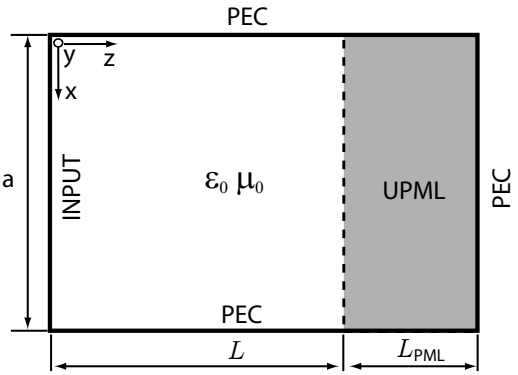

Figure 5: Rectangular waveguide: $a = 3\,cm$, $L = 5\,cm$ (not to scale).

medium has been investigated[5]. Specifically, we have evaluated the effect of the condition number[6] of $\mathbf{K}$ on the accuracy of numerical results (average ($err_{avg\%}$) and standard deviation ($\sigma_{\%}$) of the difference between the numerical results and the reference analytical solution).

As a general trend, we have observed that the wider the number of UPML elements in the z direction, the worse the conditioning of the problem, which raises the computational cost of the numerical solution. As an example, the results of a test case ($L_{PML} = 3\,cm$, $m = 2$) are presented in Table 1 together with some mesh parameters (step size Δh_z, number of primal elements n_{ele}).

Table 1: Results of a test case ($L_{PML} = 3\,cm$, $m = 2$): condition number (c), average error ($err_{avg\%}$) and standard deviation ($err_{std\%}$) of the numerical results compared to the reference analytical solution, for different values of the step size Δh_z and number of primal elements n_{ele} of the mesh.

$\Delta h_z\,[mm]$	n_{ele}	c	$err_{avg\%}$	$err_{std\%}$
2.0	1456	6.85e+07	2.94	1.97
1.0	5652	1.15e+08	0.85	0.60
0.5	22508	2.25e+08	0.34	0.25

[5] Notice that since the mesh is unstructured, we need to refer to an average step size in the z direction.

[6] The quantity $c = ||\mathbf{K}||\,||\mathbf{K}^{-1}||$ is called the condition number of $\mathbf{K}$ with respect to inversion. If we use the 2-norm, the condition number is simply the ratio of the largest singular value of $\mathbf{K}$ to the smallest.

Then, though the problem is intrinsically 2D (plane symmetry), it has been solved in a 3D numerical domain D (the height of the waveguide has been set to $b = 2\,cm$): a pair of interlocked grids has been introduced, the *primal* is tetrahedral, while the dual is obtained by the primal grid by barycentric subdivision. As an example the outer elements (triangular faces) of a coarse mesh of about $50,000$ tetrahedra are shown in Fig. 6.

The electric and magnetic tensors have been constructed according to (7), for the simplest case of a wave normally impinging on the interface (planar surface at $z = L$) between the isotropic medium and the UPML medium.

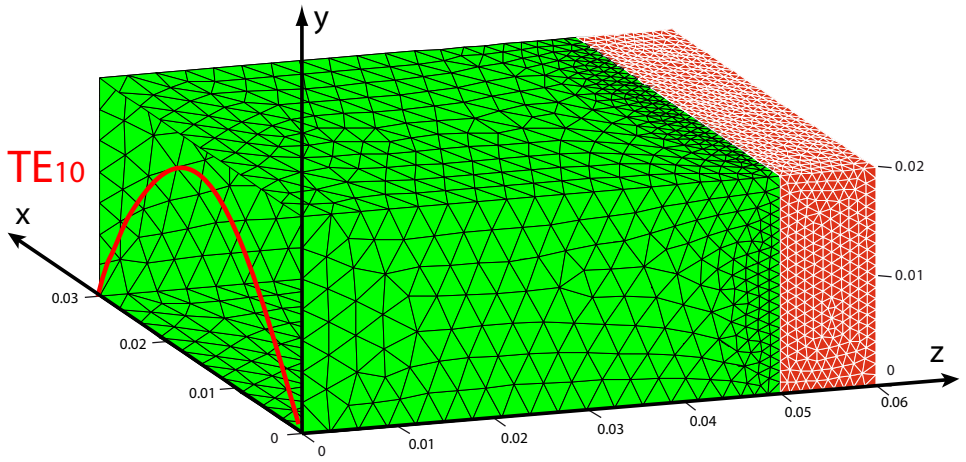

Figure 6: Numerical domain D of a rectangular waveguide (width $a = 3\,cm$, height $b = 2\,cm$, length $L = 5\,cm$) fed at one side by an electric source equivalent to the TE_{10} mode. The outer elements (triangular faces) of a coarse mesh of about $50,000$ tetrahedra are shown (not to scale).

The amplitude of the electric field evaluated at a cut plane ($y = 1\,cm$) is shown in Fig. 7.

Fig. 8 shows an almost linear dependance of the average error of the numerical results (electric E and magnetic H field components), compared to the reference solution, upon the number of primal elements n_{ele} of the mesh, which span from about $50,000$ tetrahedra for the most coarse mesh to about $200,000$ tetrahedra for the finest mesh. In this case the results are encouraging, even in the worst case (coarse mesh), but this is a fairly simple problem since the wave is purely propagating and is normally incident on the PML.

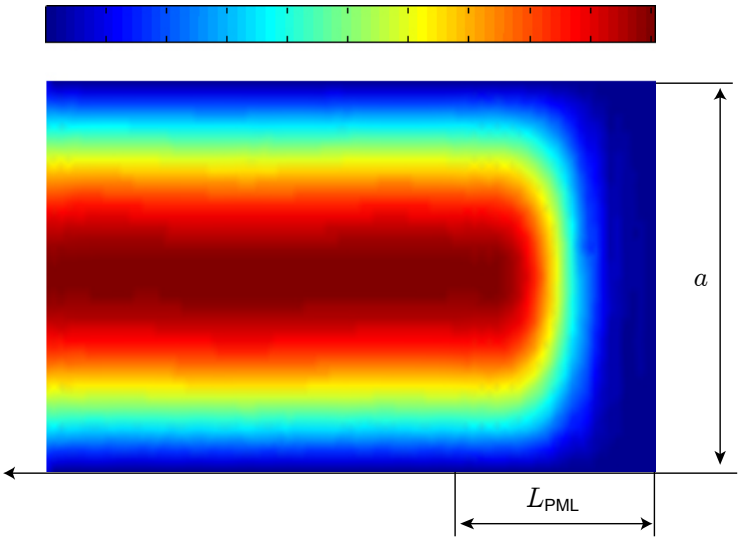

Figure 7: Amplitude of the electric field evaluated at a cut plane ($y = 1\,cm$).

3.2 $\lambda/2$ *linear antenna*

To asses the effectiveness of the proposed formulation, a more demanding 3D unbounded problem has been considered, consisting in the numerical evaluation of the Poynting vector flux across a number of nested surfaces containing a $\lambda/2$ linear antenna, fed at $f = 10\,GHz$, embedded in air.

The electric and magnetic tensors have been constructed according to (7), subdividing the numerical domain D into an isotropic inner subregion and 26 outer boundary subregions, as previously described.

The algorithms were implemented in C++ and run on a 2.1GHz Intel Core 2 Duo processor with 3GB RAM. The construction of the matrices and the solution of (3) required $12.7\,s$ and $97\,s$, respectively. A state of the art direct solver (Pardiso) from Intel Math Kernel Library (MKL) is used to solve efficiently the sparse linear system of equations.

The percentage error between numerical and reference values is fairly constant among different surfaces ($\varepsilon_{\%} < 2\%$), using a primal mesh of about $220,000$ tetrahedra and $275,000$ primal edges.

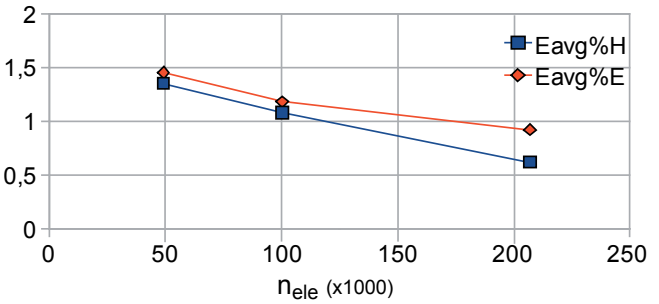

Figure 8: Average error ($err_{avg\%}$) of the numerical results (electric E and magnetic H field components) compared to the reference analytical solution.

4 Conclusions

A geometric formulation for 3D wave propagation problems in the frequency domain has been developed and successfully applied to unbounded problems, by exploiting UPML absorbing BCs over an unstructured mesh, which is a key factor in modeling complex 3D geometries. Moreover, the proposed formulation can easily handle almost any kind of material properties, including anisotropies, so that the implementation of UPML into a numerical code has been straightforward and particularly efficient. A state-of-the-art direct solver has been used to solve efficiently the sparse linear system of equations, but other solvers for sparse symmetric matrices are under investigation, mainly based on iterative schemes such as COCG (Conjugate Orthogonal Conjugate Gradient) algorithms, to allow the solution of 3D problems with over hundred millions of DoFs.

Acknowledgement: The authors are grateful to M.Sc. Michele Giorgiutti for developing, testing, and running the preliminary version of the computer software.

References

Bayliss, A.; Gunzburger, M.; Turkel, E. (1982): Boundary conditions for the numerical solution of elliptic equations in exterior regions. *SIAM J. Applied Math.*, vol. 42, pp. 430–451.

Bayliss, A.; Turkel, E. (1980): Radiation boundary conditions for wave-like equations. *Comm. Pure Appl. Math.*, vol. 23, pp. 707–725.

Berenger, J. P. (1996): Three-dimensional perfectly matched layer for the absorption of electro-magnetic waves. *J. Comput. Phys.*, vol. 127, pp. 363–379.

Bettini, P.; Boscolo, S.; Specogna, R.; Trevisan, F. (2006): A Geometric Approach for Wave Propagation in 2-D Photonic Crystals in The Frequency Domain. *IEEE Trans. Mag.*, vol. 42, pp. 827–830.

Bossavit, A. (1998): *Computational Electromagnetism*. Academic Press.

Bossavit, A. (1998): How weak is the weak solution in finite elements methods? *IEEE Trans. Mag.*, vol. 34, pp. 2429–2432.

Bossavit, A. (2000): Computational electromagnetism and geometry. (5): The galerkin hodge. *J. Japan Soc. Appl. Electromagn. & Mech.*, vol. 8, pp. 203–209.

Bossavit, A.; Kettunen, L. (2000): Yee-like schemes on staggered cellular grids: A synthesis between fit and fem approaches. *IEEE Trans. Mag.*, vol. 36, pp. 861–867.

Chew, W. C.; Weedon, W. H. (1994): A 3-d perfectly matched medium from modified maxwell's equation with stretched coordinates. *Microwave Optical Technol. Lett.*, vol. 7, no. 13, pp. 599–604.

Cinalli, M.; Edelvik, F.; Schuhmann, R.; Weiland, T. (2004): Consistent material operators for tetrahedral grids based on geometrical principles. *International Journal of Numerical Modelling*, vol. 17, pp. 487–507.

Codecasa, L.; Specogna, R.; Trevisan, F. (2007): Symmetric Positive-Definite Constitutive Matrices for Discrete Eddy-Current Problems. *IEEE Trans. on Mag.*, vol. 43, pp. 510–515.

Codecasa, L.; Specogna, R.; Trevisan, F. (2008): Discrete constitutive equations over hexahedral grids for eddy-current problems. *CMES: Computer Modeling in Engineering & Sciences*, vol. 31, no. 3, pp. 129–144.

Codecasa, L.; Specogna, R.; Trevisan, F. (2009): Base functions and discrete constitutive relations for staggered polyhedral grids. *Comput. Meth. Appl. Mech. Eng.*, vol. 198, no. 9–12, pp. 1117–1123.

Codecasa, L.; Specogna, R.; Trevisan, F. (2009): Subgridding to Solving Magnetostatics within Discrete Geometric Approach. *IEEE Trans. Mag.*, vol. 45, pp. 1024–1027.

Codecasa, L.; Specogna, R.; Trevisan, F. (2010): A new set of basis functions for the discrete geometric approach. *J. Comput. Phys.*, vol. 229, pp. 7401–7410.

Dular, P.; Hody, J.-Y.; Nicolet, A.; Genon, A.; Legros, W. (1994): Mixed Finite Elements Associated with a Collection of Tetrahedra, Hexahedra and Prisms. *IEEE Trans. on Mag.*, vol. 40, pp. 2980–2983.

Dular, P.; Specogna, R.; Trevisan, F. (2008): Constitutive matrices using hexahedra in a discrete approach for eddy currents. *IEEE Trans. on Mag.*, vol. 44, pp. 694–697.

Engquist, B.; Majda, A. (1977): Adsorbing boundary conditions for the numerical simulation of waves. *Mathematics of Computation*, vol. 31, pp. 629–651.

Higdon, R. (1986): Adsorbing boundary conditions for difference approximations to the multi-dimensional wave equation. *Mathematics of Computation*, vol. 47, pp. 437–459.

Higdon, R. (1987): Numerical adsorbing boundary conditions for the wave equation. *Mathematics of Computation*, vol. 49, pp. 65–90.

Jin, J. (1993): *The Finite Element Methods in Electromagnetics*. Wiley Interscience, New York.

Liao, Z.; Wong, H.; Yang, B.; Yuan, Y. (1984): A transmitting boundary for transient wave analyses. *Scientia Sinica*, vol. 27, pp. 1063–1076.

Marrone, M. (2001): Computational aspects of the cell method in electrodynamics. *PIER*, vol. 32, pp. 317–356.

Ramahi, O. (1997): The complementary operators method in fdtd simulations. *IEEE Antennas and Propagation Magazine*, vol. 39, pp. 33–45.

Ramahi, O. (1998): The concurrent complementary operators method for fdtd mesh truncation. *IEEE Trans. Antennas and Propagation*, vol. 46, pp. 1475–1482.

Rappaport, C. (1995): Perfectly matched adsorbing boundary conditions based on anisotropic lossy mapping of space. *IEEE Microwave and Guided Wave Letters*, vol. 5, pp. 90–92.

Sacks, Z. S.; Kingsland, D.; Lee, R.; Lee, J.-F. (1995): A perfectly matched anisotropic absorber for use as an absorbing boundary condition. *Antennas and Propagation, IEEE Transactions on*, vol. 43, no. 12, pp. 1460 – 1463.

Specogna, R.; Trevisan, F. (2005): Discrete constitutive equations in $A - \chi$ geometric eddy-current formulation. *IEEE Trans. Mag.*, vol. 41, pp. 1259–1263.

Taflove, A. (1995): *Computational Electrodynamics: The Finite-Difference Time-Domain Method*. Artech House, Norwood, MA.

Tarhasaari, T.; Kettunen, L.; Bossavit, A. (1999): Some realizations of a discrete Hodge operator: a reinterpretation of finite element techniques. *IEEE Trans. on Mag.*, vol. 35, pp. 1494–1497.

Teixeira, F. L.; Chew, W. C. (1999): Lattice electromagnetic theory from a topological viewpoint. *Journal of Mathematical Physics*, vol. 40, pp. 169–187.

Tonti, E. (1975): *On the formal structure of physical theories*. Quaderni dei Gruppi di Ricerca Matematica del CNR.

Tonti, E. (1988): Algebraic topology and computational electromagnetism. *IMF Conference*, pp. 284–294.

Tonti, E. (1998): Algebraic topology and computational electromagnetism. *4-th International Workshop on Electric and Magnetic Fields, Marseille (Fr) 12-15 May*, pp. 284–294.

Tonti, E. (2002): Finite formulation of electromagnetic field. *IEEE Trans. Mag.*, vol. 38, pp. 333–336.

Weiland, T. (1977): A numerical method for the solution of the eigenvalue problem of longitudinally homogeneous waveguides. *Electronics and Communication (AE)*, vol. 31, pp. 308–311.

Weiland, T. (1985): On the unique numerical solution of maxwellian eigenvalue problems in three dimensions. *Particle Accelerators*, vol. 17, pp. 227–242.

Yee, K. S. (1966): Numerical solution of initial boundary value problems involving maxwell's equations in isotropic media. *IEEE Transactions on Antennas and Propagation*, vol. 14, pp. 302–307.